Petrographic and geochemical study of Nyiragongo volcanic flows from the 2002 and 2021 eruptions: A comparative analysis

Innocent Mufungizi, Ndjate Ohanga, Jean Kabulo, Roda Bongeli, Trésor Hubert, Ridi Diakondua, Ruben Loola, Jonathan Musitu

ZIBELINE INTERNATIONAL™ PUBLISHING

ISSN: 2521-0890 (Print)
ISSN: 2521-0491 (Online)
CODEN: GBEEB6

Geological Behavior (GBR)

DOI: http://doi.org/10.26480/gbr.01.2024.01.12

RESEARCH ARTICLE

PETROGRAPHIC AND GEOCHEMICAL STUDY OF NYIRAGONGO VOLCANIC FLOWS FROM THE 2002 AND 2021 ERUPTIONS: A COMPARATIVE ANALYSIS

Innocent Mufungizi[a,b,c*], Ndjate Ohanga[a], Jean Kabulo[a,c], Roda Bongeli[a,c], Trésor Hubert[a,c], Ridi Diakondua[a,c], Ruben Loola[a,c], Jonathan Musitu[a]

[a]Earth Sciences, Faculty of Sciences and Technologies, University of Kinshasa, Kinshasa, B.P. 190 Kinshasa XI, DR Congo
[b]Pedology and Geochemistry Laboratory, University of Kinshasa, B.P. 190 Kinshasa XI, DR Congo
[c]LeGeolog Research Team, Kinshasa, DR Congo
**Corresponding Author Email: innocent.mufungizi@unikin.ac.cd*

ARTICLE DETAILS

Article History:

Received 13 December 2023
Revised 16 January 2024
Accepted 18 February 2024
Available online 06 March 2024

ABSTRACT

Context: One of the volcanoes on the East African Rift's Virunga chain is the Nyiragongo. It is recognized for its Hawaiian-style eruptive dynamism and is especially interesting for studies aimed at comprehending the dynamics of the East African Rift. **Objectives:** In order to close the geochemistry gap, comprehend the evolution of the Nyiragongo magmas over a 20-year period, and enhance our knowledge of the southern region of the Nyiragongo volcanic field, this paper examines the significance of comparative research on the petrography and geochemistry of Nyiragongo volcano flows from 2002 and 2021. **Approaches:** A field campaign was conducted using the Hammer Survey method to characterize available outcrops macroscopically. Samples were taken to identify unnoticed size and propose relative words. Four out of fifteen samples underwent microscopic examination. **Results:** The 2021 and 2002 Nyiragongo volcano eruptions have similar mineralogical compositions, dominated by nepheline phenocrysts. However, the 2021 lava has a porphyritic to microlithic texture, with undersaturated silica and enriched alkalis. Olivine microlith is present in the 2002 flow, but not in the 2021 lava. **In conclusion,** the persistence of dispersive features linked to the East African rift is demonstrated by the geochemical description of geotectonic locations. The alkaline series is geochemically suited to both flows.

KEYWORDS

Magmatic Series, Petrography, Geochemistry, Nyiragongo Volcano, East African Rift

1. INTRODUCTION

The activities of the Earth are either caused by internal or external dynamism. Since our earth is an active planet, one of the most striking examples of this activity is volcanism (Marie, 2008). This activity is characterized by the release of gas and lava as well as slightly significant projections on the lithosphere's surface that indicate the rise of magmas formed at depths to the top by way of fractures. Volcanic massifs are intricate geological formations that allow the planet to breathe by emitting gases, magma, and fluids known as hydrothermal fluids. During the same epoch, a series of eruptions formed the volcanoes, which were later largely destroyed by collapse, erosion, and explosions. Thus, it is typical to see different nested or layered structures (Siebert et al., 2011; Cole-Dai, 2010).

One of the most studied geological giga-structures in Africa is the East African Rift in the eastern part of the continent from the Gulf of Tadjoura to Lake Malawi in Mozambique crossing two oceanic rifts (Popoff, 1988; Tiercelin et al., 1989). Through the Ethiopian plateaus, the East African Rift creates a structure that stretches up to 6,000 kilometers. According to Roberts et al. (2012), it evolved as a result of internal dynamics that led to mantle plume activity. Kamate (2018) claims that whereas volcanism in the western branch is limited to the transfer zone, it is dispersed throughout the eastern branch of eastern Africa. In general, the continental crust of Africa is robust and cold. There are several cratons in the Est-African Rift, including the Tanzania and Kaapvaal cratons. Because of their thickness and lack of tectonic activity, crusts have endured for billions of years. Tonalites, metamorphic lithologies, and greenstone belts are some of their distinguishing features. With notable amounts of gold, antimony, iron, chromium, and nickel, cratons are valuable in terms of natural resources (Taylor et al., 2009). The Oligocene saw the eruption of a significant amount of continental flood basalts, with the majority of volcanism occurring approximately 30 Ma (Ebinger and Sleep, 1998), when the Red Sea and Gulf of Aden opened. Rocks formed by volcanic eruptions range in composition from ultra-alkaline to tholeiitic and felsic rocks. Various mantle source zones might account for the compositional variability. Additionally, the Est-African Rift traverses historic basins that have accumulated sedimentary materials throughout time (Saemundsson, 2009).

With two of Africa's most active erupting volcano, the western segment of the East African Rift is located in the Virunga mountains and is the most active. But the most extensive and having the greatest amount of lava deposits is the eastern branch (Hamaguchi, 1983; Mishina, 1983; Mishina et al., 1983). North of Lake Kivu, the Virunga volcanic province is situated in an area of plate uplift and extension linked to an unusually hot asthenosphere (Kamate, 2018).

The area has seen relatively minimal lithosphere expansion and partial melting, as reported by Ebinger (2002); geochemical, geophysical, and structural evidence support this conclusion. In the northern portion of the Western Rift branch, in the Toro-Ankole volcanic area, there are potassic lavas undersaturated in silica and carbonatitic tuffs with silica levels ranging from 31.8% to 42.8%, high CaO values, and K_2O exceeding 16.6% and 7%, respectively (Rosenthal, 2009). Geographic position has a

Quick Response Code	Access this article online	
	Website: www.geologicalbehavior.com	DOI: 10.26480/gbr.01.2024.01.12

Cite The Article: Innocent Mufungizi, Ndjate Ohanga, Jean Kabulo, Roda Bongeli, Trésor Hubert, Ridi Diakondua, Ruben Loola, Jonathan Musitu (2024). Petrographic and Geochemical Study of Nyiragongo Volcanic Flows from the 2002 and 2021 Eruptions: A Comparative Analysis, *Geological Behaviour 8(1): 01-12.*

systematic effect on the isotopic ratio and trace elements of the western branch, particularly the Kivu volcanic province (Furman, 1999).

One of several volcanoes on the East African Rift's Virunga range is Nyiragongo (Hirschn and Bernard, 2009). It is renowned for its Hawaiian-style eruptive dynamism (Sadaka et al., 2003) and has the biggest lava lake on Earth (Smets et al., 2017).

This volcano's outbursts have been the subject of several research. Wauthier et al. (2012) point out that there is a good chance that the deeper reservoir's magma supply started many months before the 2002 eruption, which may be explained by prolonged seismic activity. Conversely, Colclough (2005) hypothesizes that the energy that led to enormous fracture was enhanced by localized tectonic events.

A mound of lava flows supports the cities of Goma, Gisenyi (Rwanda), and the southern portion of Nyiragongo region. The southern region of the Nyiragongo volcanic field also has pyroclastic cones from earlier volcanic activity. Being among the most erupting volcanoes in the Virunga volcanic area, it constantly threatens the nearby villages and the towns of Goma and Gisenyi. At least three significant eruptions of this powerful monster have occurred in the last fifty years (1977, 2002, and 2021). According to research findings that nephelinites, melilitites, and basanites are the primary constituents of Nyiragongo (Ongendanda, 2012; Minissal et al., 2019; Badriyo et al., 2022).

A number of questions have prompted this investigation and piqued our interest in the subject's applicability. Finding commonalities between the volcanic flows from 2002 and the 2021 Nyiragongo eruption in terms of petrographic nature and chemical composition is the goal. To our knowledge, there does not appear to be adequate petrographic and geochemical information about the eruption of 2021. We selected the years 2002 and 2021 given that the almost two-decade difference enables us to comprehend the petrographic and geochemical aspects of the history of Nyiragongo volcanism. This investigation aims to clarify our understanding of the geology of the southern region of the Nyiragongo volcanic region.

2. Methodology

The administrative region of North Kivu contains the Nyiragongo volcano, which is bordered to the northwest by the regions of Masisi and Rutshuru, to the southeast by Rwanda, and to the south by the city of Goma (Figure 1).

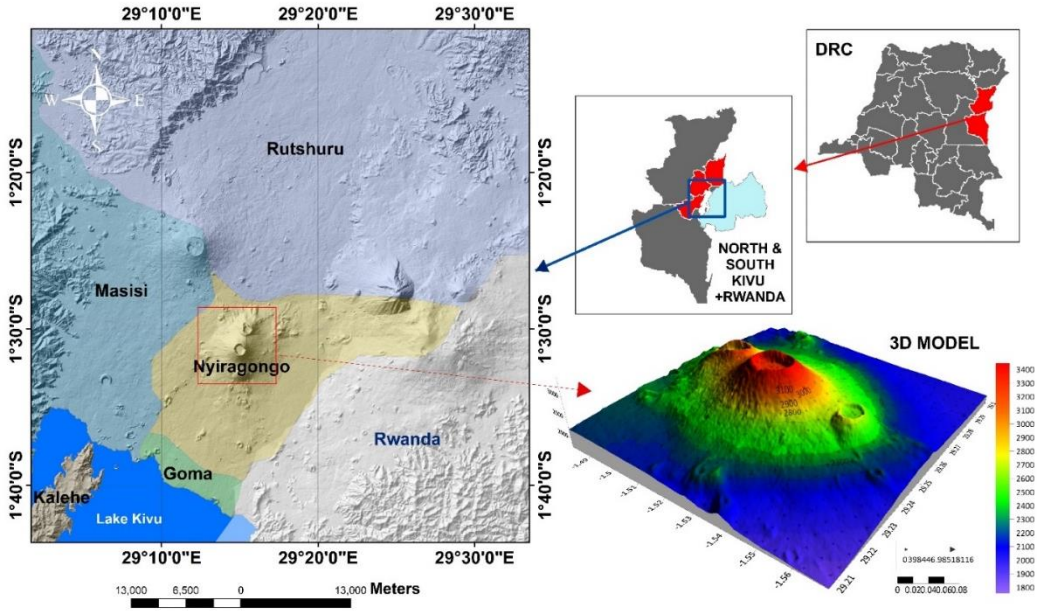

Figure 1: This research area's location is shown with a three-dimensional model of the Nyiragongo volcano.

2.1 Field work

For the field phase, we carried out a geological survey which is a field campaign during which we made macroscopic observations. Hydrology, sedimentology, geomorphology and volcanology were taken into account to make observations of the accumulations of geological materials in place. During this phase, we collected rock samples which we brought to the laboratory for geochemical analyses.

2.2 Work in A Laboratory Setting

We proceeded to the laboratory phase following the field phase. When classifying rocks using petrographic and geochemical techniques, whole rock analysis procedures are necessary. Sample melt breakdown, which releases all the elements for analysis by dissolving every element in the sample, is a component of all whole rock techniques. In order to report silica, techniques for identifying the primary rock-forming components were also used. Regarding these, we observed and described various outcrops and samples in macroscopic detail. This enabled us to gather the required data, which included the locations of various outcrops and sampling points, the identification of texture, color, and, if possible, visible minerals, the degree of alteration, and likely lithology. Throughout our field campaign, we employed the subsequent tools: a magnifying glass for the macroscopic examination of samples; a digital camera for taking images of outcrops and samples to be described; a geologist's hammer for taking samples of the rocks studied; a clinometer compass for ground orientation, and a Garmin-style GPS for finding outcrops and sampling points; an indelible marker to label samples, an observation notebook and pen to record locations and samples, sample packing, and a bag to contain every single sample.

We were able to learn more about the lithology of the areas under study, which were primarily covered by the flows of 2002, and 2021, thanks to a petrographic investigation of the samples. A polarizing microscope was used to examine the thin slices under a microscope. Overall, four samples, two based on the 2002 flow and two from 2021 were chosen for extensive examination and split into two groups. The flow samples from 2002 and 2021 were then subjected to a geochemical analysis. In order to do this, we prepared samples for geochemical analysis that examined major and trace elements as well as thin slices for microscopic investigations. In order to fulfill the requirements of our geochemistry study, we described the arrangement of elements while understanding the various chemical data obtained from the research facility in order to categorize and describe the lava released from the Nyiragongo volcano throughout the eruptions that are the focus of our investigation, in 2002 as well as 2021.

2.3 Analysis and Processing of Data

The seismic and magnetic data were downloaded to the USGS Earthquake Catalog and International Gravimetric Bureau websites. These data were then processed by GIS tools. In order to classify the magmatic series geochemically and assess their evolutionary tendency, the collected geochemical data were examined applying geochemical information-processing tools. Additionally, we employed computerized geographic information system technologies and spatial analysis to create a map of volcanic flows for the years 2002 and 2021 based on the data collected in the field during the study.

3. Results and Discussion

3.1 Seismic Activities

Frequently, an earthquake signals the impending eruption. The pressure in the rocky materials is caused by the increasing motions of magma. An

eruption is likely due to the volcano's waking phase, as evidenced by the hypocenters' increasing elevation, which is correlated with the magma's ascent. This results in gas releases, crustal swelling, cracking, and earthquakes. Volcano monitoring in the city of Goma is the responsibility of the volcanological observatory. Seismic data for the area is shown in the following table.

Table 1: *Seismic data from 2000 to 2024*

Time	Depth	Magnitude	Place
2002-01-17T14:26:59.720Z	10	4.3	9 km WNW of Goma, Democratic Republic of the Congo
2002-01-17T20:01:29.260Z	15.4	4.7	12 km SSE of Sake, Democratic Republic of the Congo
2002-01-18T08:07:57.370Z	10	4.2	1 km WSW of Sake, Democratic Republic of the Congo
2002-01-18T15:14:02.040Z	10	4.3	20 km SW of Goma, Democratic Republic of the Congo
2002-01-18T21:08:53.320Z	10	4.2	22 km WSW of Sake, Democratic Republic of the Congo
2002-01-19T04:26:20.490Z	10	3.9	22 km SSW of Sake, Democratic Republic of the Congo
2002-01-19T17:09:29.170Z	10	4.6	25 km W of Eglise Catholique, Centrale GIKO, Rwanda
2002-01-19T20:38:55.550Z	10	4.2	29 km SW of Gisenyi, Rwanda
2002-01-20T00:14:44.390Z	10	5.1	13 km SSW of Sake, Democratic Republic of the Congo
2002-01-20T05:17:19.580Z	10	3.9	7 km S of Sake, Democratic Republic of the Congo
2002-01-20T23:28:17.470Z	10	4.2	2 km SSE of Sake, Democratic Republic of the Congo
2002-01-20T23:31:45.480Z	10	3.8	8 km SW of Goma, Democratic Republic of the Congo
2002-01-21T01:19:32.600Z	10	4.6	26 km SW of Sake, Democratic Republic of the Congo
2002-01-21T02:00:14.000Z	10	4.2	13 km NW of Sake, Democratic Republic of the Congo
2002-01-21T04:39:21.620Z	10	5.1	22 km S of Sake, Democratic Republic of the Congo
2002-01-21T10:55:03.720Z	10	4.7	27 km SW of Gisenyi, Rwanda
2002-01-22T01:02:32.250Z	10	4	24 km SSW of Sake, Democratic Republic of the Congo
2002-01-22T02:01:01.340Z	10	3.9	16 km WSW of Goma, Democratic Republic of the Congo
2002-01-22T15:32:05.590Z	10	5.2	8 km NW of Sake, Democratic Republic of the Congo
2002-01-22T16:22:22.340Z	10	4.4	5 km WNW of Sake, Democratic Republic of the Congo
2002-01-22T16:51:00.380Z	10	4.2	23 km N of Goma, Democratic Republic of the Congo
2002-01-30T00:33:09.140Z	10	4.6	18 km WSW of Sake, Democratic Republic of the Congo
2002-02-11T13:49:26.120Z	10	4.4	21 km N of Sake, Democratic Republic of the Congo
2002-10-24T06:08:37.980Z	11	6.2	34 km SW of Goma, Democratic Republic of the Congo
2002-10-24T07:12:18.400Z	10	5.5	28 km SSW of Sake, Democratic Republic of the Congo
2002-10-26T12:56:47.710Z	10	4.7	12 km E of Sake, Democratic Republic of the Congo
2002-12-13T13:24:25.940Z	10	4.7	28 km SW of Goma, Democratic Republic of the Congo
2003-08-22T22:06:50.090Z	10	4.3	33 km SW of Gisenyi, Rwanda
2006-11-27T17:49:50.820Z	10	3.8	11 km NE of Sake, Democratic Republic of the Congo
2008-10-05T00:32:10.620Z	10	4	19 km NNE of Sake, Democratic Republic of the Congo
2021-05-22T23:54:55.994Z	10	4.3	7 km SW of Gisenyi, Rwanda
2021-05-23T13:07:55.737Z	10	4.5	18 km SE of Gisenyi, Rwanda
2021-05-23T16:52:25.489Z	13.06	4.3	24 km SE of Gisenyi, Rwanda
2021-05-23T20:38:56.907Z	10	4.5	2 km NNE of Goma, Democratic Republic of the Congo
2021-05-23T22:52:56.472Z	10	4.3	17 km ENE of Gisenyi, Rwanda
2021-05-24T08:37:25.450Z	10	4.7	9 km N of Goma, Democratic Republic of the Congo
2021-05-25T08:19:55.526Z	10	4.5	15 km ESE of Gisenyi, Rwanda
2021-05-25T09:03:00.255Z	10	4.7	19 km WSW of Musanze, Rwanda
2021-05-25T09:41:17.053Z	10	4.4	9 km SE of Gisenyi, Rwanda
2021-05-25T10:40:45.451Z	10	4.3	16 km ESE of Gisenyi, Rwanda
2021-05-25T12:16:27.112Z	10	4.4	5 km S of Gisenyi, Rwanda
2021-05-25T20:38:11.781Z	10	4.3	18 km ENE of Gisenyi, Rwanda
2021-05-26T03:46:31.637Z	10	4.7	16 km E of Gisenyi, Rwanda
2021-05-26T07:01:18.009Z	10	4.2	28 km ESE of Gisenyi, Rwanda
2021-05-26T08:51:59.394Z	10	4.4	1 km SSW of Gisenyi, Rwanda
2021-05-26T11:41:18.641Z	10	4.4	8 km NE of Gisenyi, Rwanda
2021-05-26T16:07:17.587Z	10	4.5	9 km SE of Gisenyi, Rwanda
2021-05-26T17:32:56.193Z	12.65	4.5	4 km S of Gisenyi, Rwanda
2021-05-26T23:19:33.292Z	12.91	4.5	11 km SE of Gisenyi, Rwanda
2021-05-26T23:26:58.082Z	12.86	4.5	17 km SSE of Gisenyi, Rwanda
2021-05-27T03:23:52.234Z	10	4.3	17 km ENE of Gisenyi, Rwanda
2021-05-27T09:33:54.317Z	10	4.5	14 km E of Gisenyi, Rwanda

The active dynamism of the East African Rift is signified by the seismic activity represented in the Figure 2. This figure presents the spatial distribution of earthquakes from 2000 to 2024.

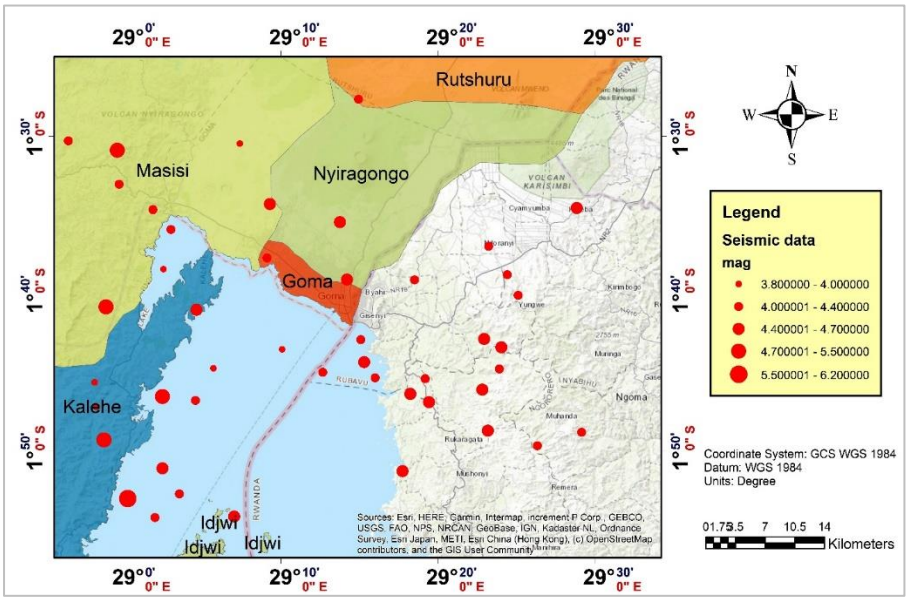

Figure 2: Spatial distribution of seismic activities from 2000 to 2024

Seismic activities were recorded in 2002 with strong repetition. 27 activities were recorded with magnitudes ranging from 3.8 to 6.2 with an average of 4.5. In the interval from 2002 to 2021, activities were recorded in 2003, 2006 and 2008 with magnitudes of 4.3, 3.8 and 4 respectively. In 2021, there were again repetitive seismic activities. 22 activities were recorded with magnitudes ranging from 4.2 to 4.7 with an average of 4.44 (Figure 3).

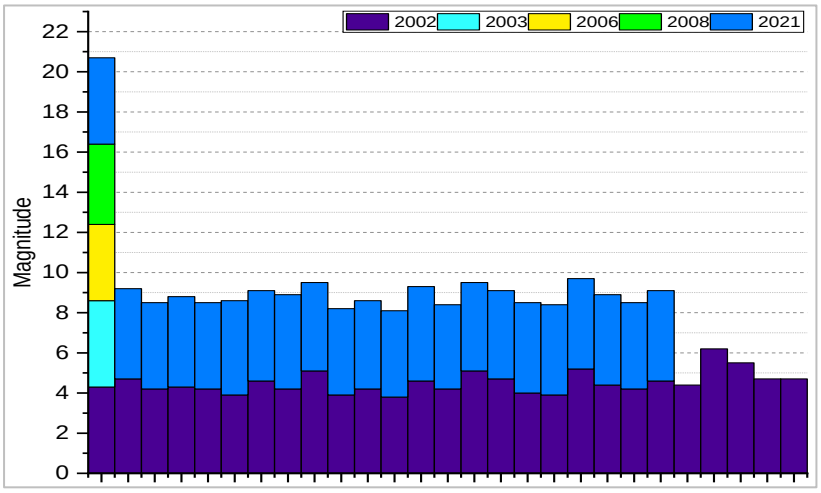

Figure 3: Variation in the magnitude of seismic activities from 2000 to 2024 in the study area

3.2 An Assessment of The Volcanic Flows

The Nyiragongo volcano has a 180-meter-long lava channel that has a 7° slope that links the eastern margin of its lava lake to the projection cone. The slope facilitates flow over eruptions, but as a result of strong degassing and visibility obstructions, it is challenging to estimate this flow (Burgi et al., 2020). Nevertheless, semicircular channels and slopes were taken into consideration by authors Jeffreys (1925), Lev, and James (2014) when estimating the flow of lava. According to calculations made for pahoehoe lava, the projected value of 4 m3/s falls into the range of volumetric rates of flow (Rowland and Walker, 1990; Gregg, 2017). We acquired then examined the condition of the volcanic cone before to the eruptive stages utilizing the services of the Google Engine. The conditions of the Nyiragongo volcanic cone before to the 2002 eruption are shown in Figure 4a, and the conditions prior to the 2021 eruption are shown in Figure 4b.

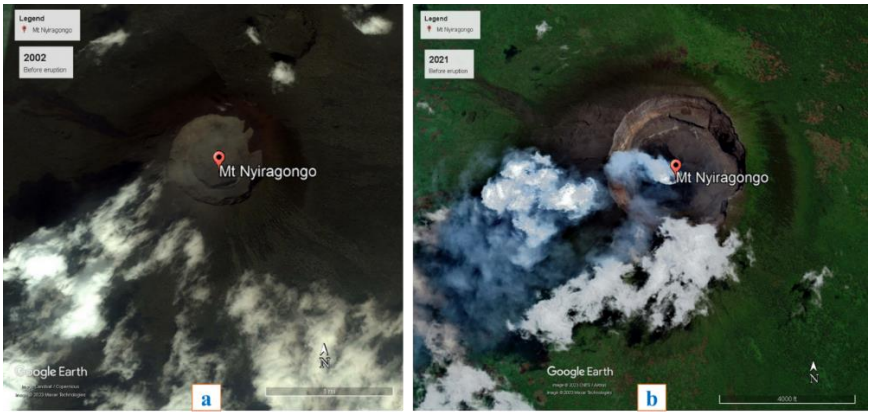

Figure 4: a) An illustration of the Nyiragongo volcanic cone's condition earlier than the eruption in 2001; b) An illustration of the volcanic cone prior to its eruption in 2021.

We collected rock samples for laboratory analysis and conducted microscopic examinations over the field expedition. The sample map and the Nyiragongo volcanic flows from 2002 and 2021 are shown in Figure 5. We observe that the 2002 floods passed via Goma and ended up to the waters of Lake Kivu.

The lava flows on the surface taking advantage of the topography of the environment and descends towards the city at a precise speed. The topographical data of the area, after statistical processing, present the parameters shown in the following table 2 while the following figure presents the topographical data processed by the geographic information system tools.

The following figure shows some sample field pictures. We see the following: the advanced front of the 2021 lavas on top of the 2002 lavas; the overlapping of the two lavas (a); and the lava flow from the May 22, 2021 eruption, which collides with the 2002 emission's (c). Some plants are present on the 2002 flow, but the current flow has yet to be conducive to the growth of the vegetation.

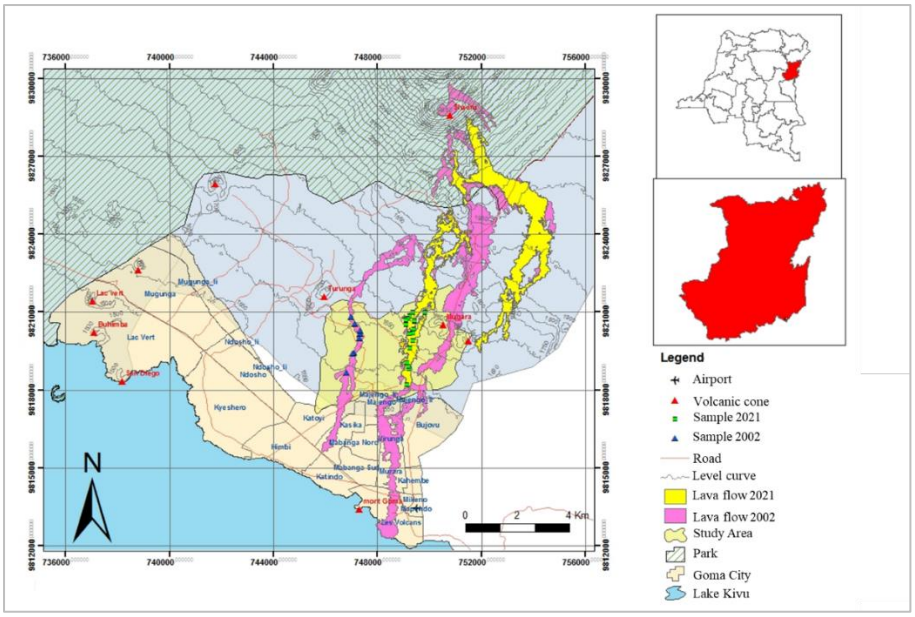

Figure 5: Map of sampling stations displaying the volcanic flows from Nyiragongo in 2002 as well as 2021.

Table 2: Statistical parameters of topographic data (altitude) of the study area

Parameter	Value	Parameter	Value	Parameter	Value
Count:	6300	Mean:	2454.74702	Variance:	104596.332
		Median:	2354.32407	Standard Deviation:	323.413563
1%-tile:	1991.69559	Geometric Mean:	2434.8009	Interquartile Range:	447.949806
5%-tile:	2083.28136	Harmonic Mean:	2416.16739	Range:	1432.86573
10%-tile:	2136.24095	Root Mean Square:	2475.95691	Mean Difference:	353.641718
25%-tile:	2202.45466	Trim Mean (10%):	2434.04905	Median Abs. Deviation:	182.23043
50%-tile:	2354.31412	Interquartile Mean:	2379.01696	Average Abs. Deviation:	252.213113
75%-tile:	2650.40446	Midrange:	2679.10912	Quartile Dispersion:	0.09230637
90%-tile:	2953.46101	Winsorized Mean:	2442.31449	Relative Mean Diff.:	0.14406443
95%-tile:	3130.06592	TriMean:	2390.37184		
99%-tile:	3330.69782	Sum:	15464906.2	Standard Error:	4.07462789
		Sum Absolute:	15464906.2	Coef. of Variation:	0.13175026
Minimum:	1962.67626	Sum Squares:	3.8621E+10	Skewness:	0.93837391
Maximum:	3395.54199	Mean Square:	6130362.64	Kurtosis:	3.08773613

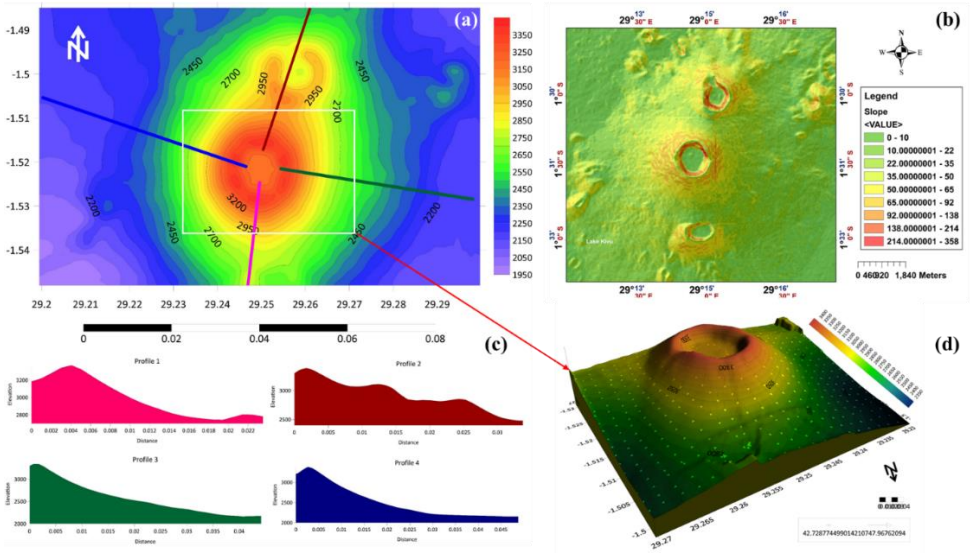

Figure 6: Topographic map of area (a); slope map of the area in percentage (b); topographic profiles (c): profile 1 (NS), profile 2 (SN), profile 3 (WE) and profile 4 (EW); 3D model of the main crater of the Nyiragongo volcano with contour lines and flow symbols.

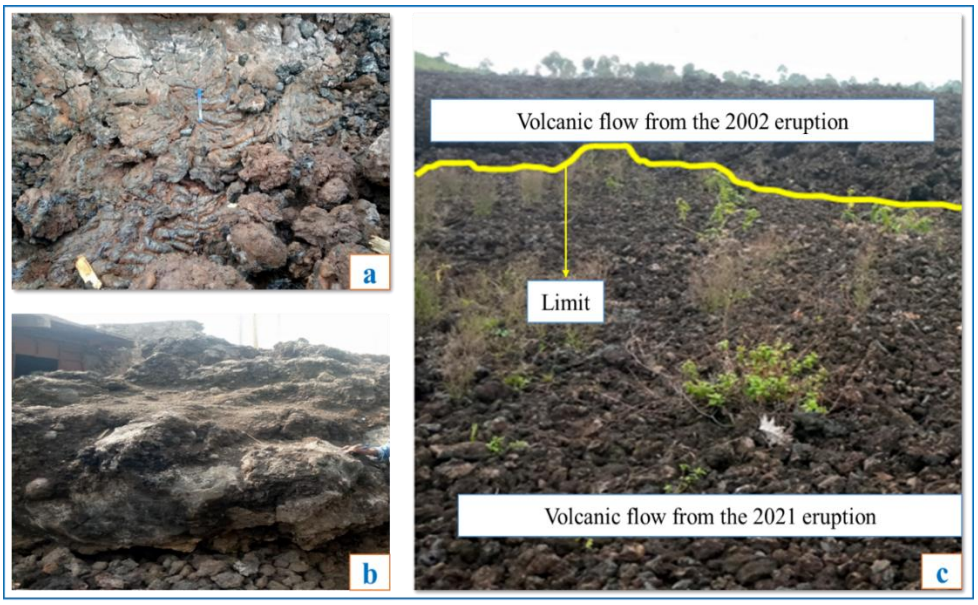

Figure 7: a) Corded lavas superposed; b) 2021 lava pushing ahead of 2002 lava; c) 2021 flows of lava physically contacting 2002 flows of lava.

3.3 Petrographic analysis

Based on a macroscopic perspective, the characteristics that follows were noted: the material's coloring varies from dark to gray; it has cavities and vacuoles at the surface; rock outcrops have an aphanitic texture; AA, corded, and pahoehoe type flows are highlighted; some areas have slag; the rocks are arranged in layers on top of one another; the flows recognized as occurring in 2002 are submerged by those determined as a result of the volcanic eruption in 2021. In macroscopic perspective, sample ND02 for the 2021 flows has a large structure that is thick and rigid. The minerals that make up this structure are not readily apparent to the unaided eye, making it aphyric and gray in hue. When examined under a microscope, this rock was found to be vacuolar, harshly, thick, and roughly compact. It is pale in hue, black, and composed of a few plagios of phenocrysts. The vitreous sheen is imbedded in the vitreous matrix. The samples' texture is porphyritic, and nephelines are the most common phenocrysts in the material. Additionally, opaque oxides are noted. Glass, or the non-crystallized portion, is what makes up the mesostasis. The nepheline phenocrysts found in the rock exhibit mild birefringence and a brilliant hue in LPA, but they are colorless in LPNA. Nephelines are more common in rocks and have xenomorphic phenocrysts. In LPNA, these crystals exhibit colorlessness and a relatively poor cleavage, but in LPA, they have weak birefringence and a polarization hue that is quite dark gray. There, an erratic extinction is noted. Overall, the cleavage is rather weak. Given the aforementioned features, it is feasible to conclude that nepheline predominates in the composition of minerals of the two samples from the 2021 flow (Figure 8). It is important to consider the following paragenesis in light of the primary minerals' interactions: Very little amounts of olivine, feldspathoids (nepheline), and high-temperature plagioclase were the next minerals to crystallize. These were the ferromagnesian and opaque minerals that would make up the mesostasis stage.

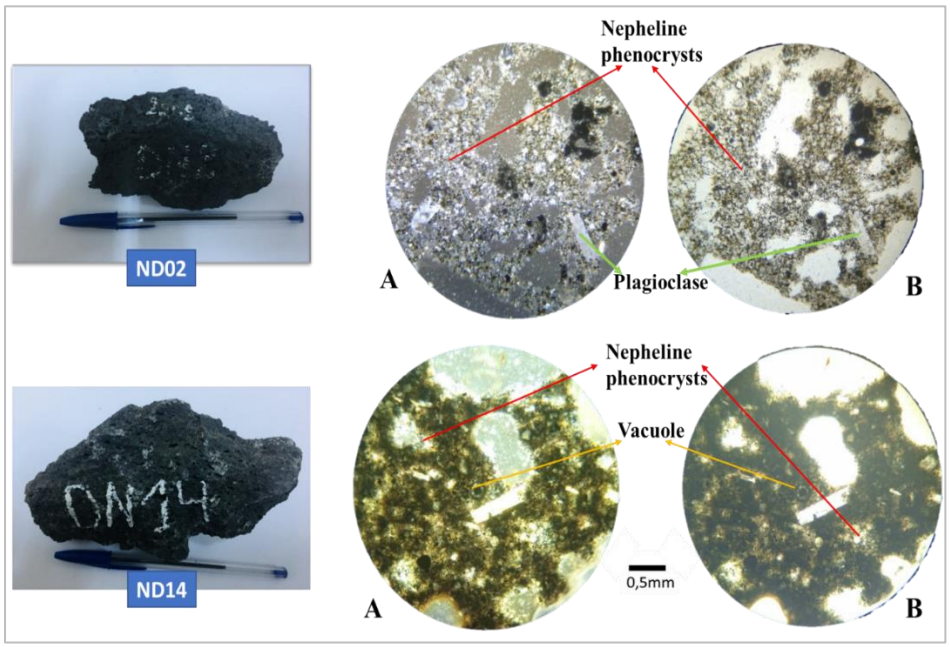

Figure 8: A brief overview of a few common rock pieces from the flow of the 2021 eruption.

Sample ND4 for the 2002 flows is black, compact, thick, and hard, with a few tiny, spherical vacuoles present. The minerals that make up the rock are invisible at the macroscopic level, making the rock wholly composed of matrix (aphyric). The material is vacuolar, hard, thick, and roughly compact. It is likewise black, consisting of a few white-colored plagio phenocrysts embedded in the vitreous matrix that have a vitreous sheen. Sample ND6 is composed of a few plagios of phenocrysts and is black in color. It is somewhat dense and has a vacuole (Figure 9). As a result, we observe that the 2021 flows and the 2002 flows are petrographically comparable. Both of the rocks are basalts.

3.4 The Geochemical Analysis

The subsequent information is included in Table 3. The geochemistry of the most important components results is as follow: two recent eruptions have demonstrated a high potassium geochemical affinity; the silica content varies between 38.85 and 40.56%; the high K_2O content fluctuates between 5.21 and 5.25; the high Na_2O content fluctuates between 5.4 and 5.53; and the low MgO contents (2.7–4.18) have also been observed.

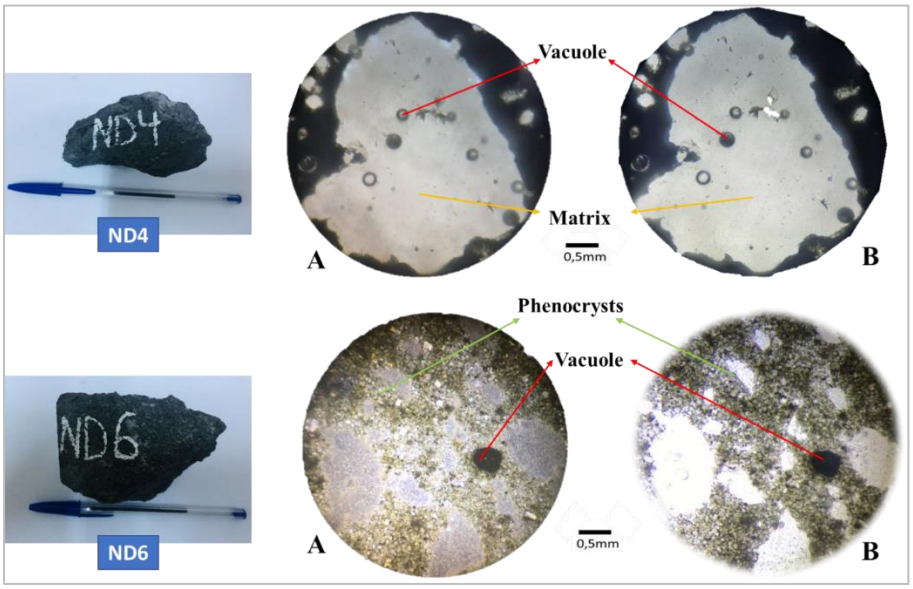

Figure 9: Microscopic overview of a few common rock fragments of the flow of the 2002 eruption.

Table 3: Percentage-based geochemical data concerning the main components of the Nyiragongo volcanic flows in 2002 and 2021.

2002					2021				
OXYDES	DN005	ND006	ND007	ND008	OXYDES	ND001	ND002	ND003	ND004
SiO_2	39.8	39.91	39.5	39.5	SiO_2	39.31	38.85	39.15	40.56
TiO_2	2.87	2.85	2.88	2.88	TiO_2	2.79	2.87	2.88	2.14
Al_2O_3	14.69	14.67	14.71	14.71	Al_2O_3	14.82	14.96	14.94	19.49
Fe_2O_3	13.7	13.64	13.68	13.68	Fe_2O_3	13.48	13.82	13.71	10.56
MnO	0.29	0.29	0.3	0.3	MnO	0.29	0.27	0.3	0.24
MgO	4.14	4.15	4.18	4.18	MgO	4.08	4.15	3.97	2.77
Cao	12.27	12.3	12.33	12.33	Cao	11.71	12.11	11.63	9.04
Na_2O	5.4	5.45	5.53	5.53	Na_2O	5.71	5.5	5.65	6.43
K_2O	5.25	5.22	5.21	5.21	K_2O	5.21	5.32	5.28	7.54
P_2O_5	1.52	1.49	1.49	1.49	P_2O_5	1.49	1.47	1.5	1.05
TOT	99.93	99.97	99.81	99.81	TOT	98.89	99.32	99.01	99.82

According to Figure 10, which displays the normative composition of lava resulting from two recent eruptions by Nyiragongo, the lavas of 2002 and 2021 are rich in feldspathoids, with a differentiation index ranging from 49.749 to 51.063%. Given that this index is high and strongly associated with SiO_2, we may conclude that differentiation occurred in the magma prior to the lavas' surface formation, explaining their highly developed nature. These lavas did not originate directly from the original magma, as evidenced by their low MgO concentrations (2.7–4.18), which indicates that the magma's chemical composition changed throughout the magmatic ascent. When the MgO level is between 8 and 15% and in balance with the mantle's olivine, a magma is considered primary (Chazot et al., 2017; Sambo et al., 2016).

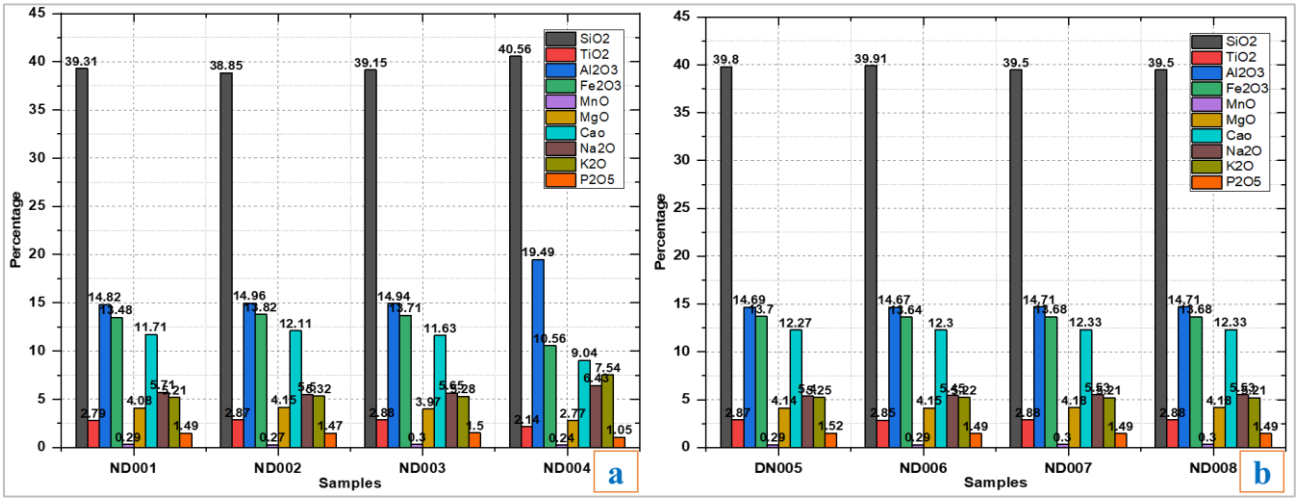

Figure 10: Nyiragongo lavas' normative composition is as follows: a) 2021; b) 2002

It should be noted that Sr and Ba are the most predominant trace elements with values respectively up to 2769 and 2430 ppm for samples from the 2002 flows and 5669 and 2340 ppm for samples from the 2021 flows. Table 4 displays the results that were obtained from the trace element analysis.

3.4.1 The Magma Series' Chemical Categorization

The casting samples from the 2002 and 2021 eruptions comply with the faiths, according to the use of chemical data in the TAS (Total Alkali and Silica) categorization diagram of Le Bas et al. (1986) and Middlemost (1994). Based on the modal chemistry of the samples studied, Le Bas et al. (1986) and Middlemost (1994) noticed that the lavas produced by the Nyiragongo volcano are Foidites, and the distribution of alkalis (Na_2O + K_2O) in relation to silica (SiO_2) confirms this. All of the lavas show up in the Foidite zone in the diagram. The lavas of 2002 and 2021 (Figure 11) released by the Nyiragongo are alkaline and insufficiently saturated in silica, according to the TAS diagram of Le Bas et al. (1986), Middlemost (1994). The K_2O concentration falls progressively as the SiO_2 content increases, whereas the Na_2O value approaches that of K_2O.

Table 4: Trace amounts, given as parts per million, from the Nyiragongo volcanic flows in 2002 and 2021									
2002					**2021**				
OXYDES	ND005	ND006	ND007	ND008	OXYDES	ND001	ND002	ND003	ND004
Cr	3.3	3.1	3.5	3.4	Cr	3.6	3.3	2.9	3
Ni	35	32	28	30	Ni	33	32	36	31
Rb	140	136	147	143	Rb	143	142	145	170
Sr	2744	2680	2769	2675	Sr	5669	2675	2701	2181
Y	40	38	40	39	Y	38	40	42	32
Zr	345	333	339	335	Zr	330	320	315	281
Nb	258	260	258	261	Nb	268	263	259	251
Ba	2296	2295	2430	2317	Ba	2302	2340	2326	2059
La	189	191	188	187	La	188	190	185	188
Ce	334	328	329	330	Ce	335	330	329	329

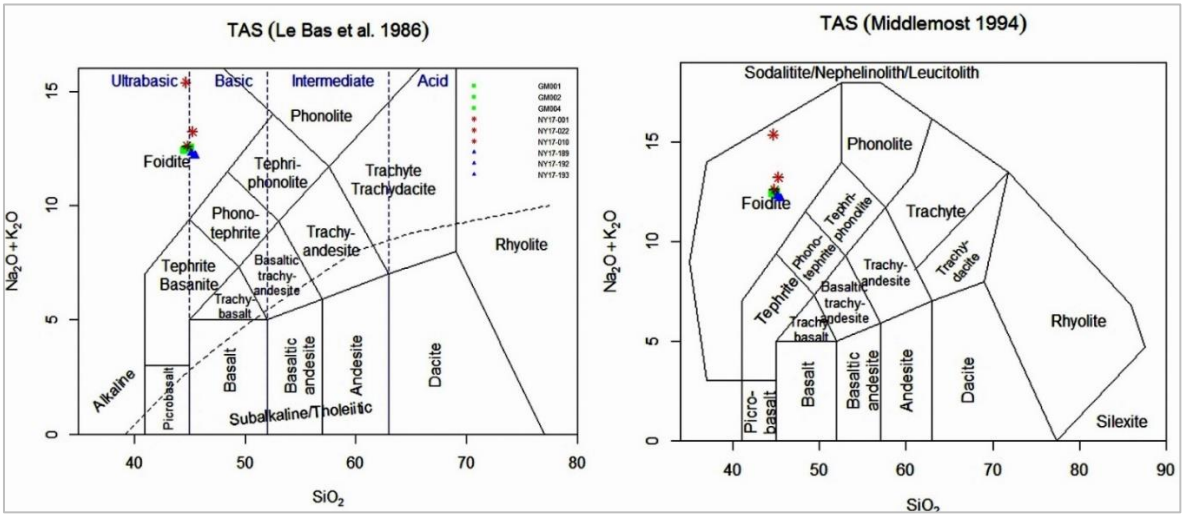

Figure 11: Diagrams showing the magmatic series' chemical categorization as per Le Bas et al. (1986) and Middlemost et al. (1994). The 2002 samples are represented by the blue representations, and the 2021 lavas by the green ones.

These observations are confirmed by the two diagrams that follow in Figure 12. R1-R2 Volcanic Chemical Variation Diagram. This comprises the level of silica saturation, a mineralogical system, all of the main cations, and the overall shifts in Fe (Fe+Mg) and (Ab+Or) (De la Roche et al., 1980) and Volcanic Rock Classification based on the modal and normative composition proposed by the authors Enrique and Esteve in 2019.

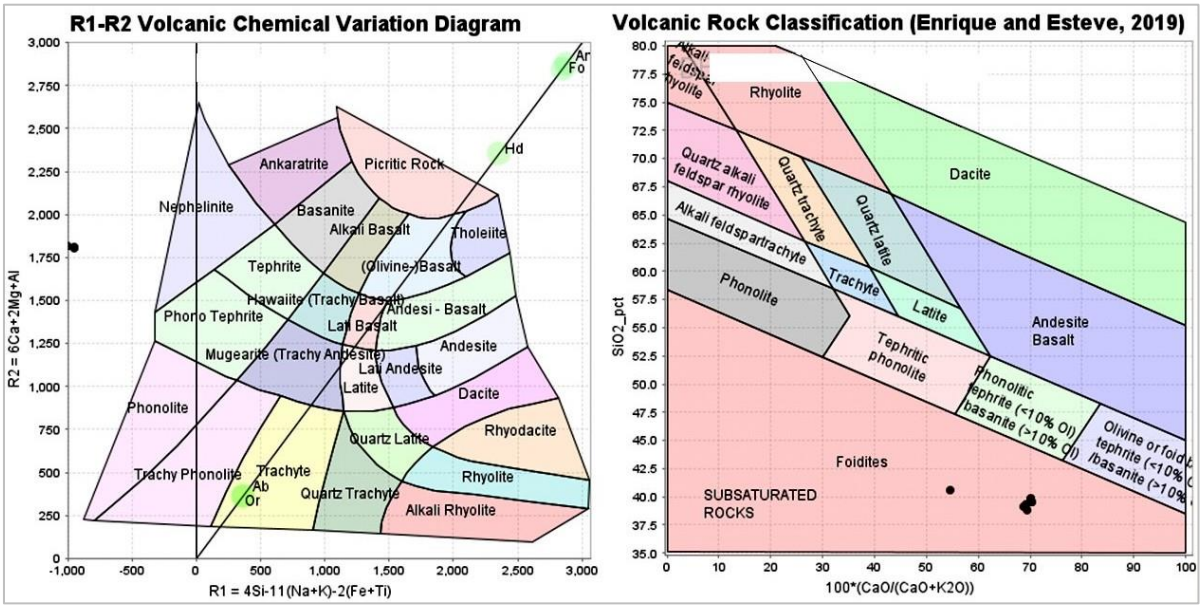

Figure 12: R1-R2 Volcanic Chemical Variation Diagram and Volcanic Rock Classification

3.4.2 Oxides' Evolutionary Tendency

According to the variation diagrams of the principal elements in connection to silica, the geochemical development (Figure 13) demonstrates that oxides like TiO_2, CaO, MgO, and Fe_2O_3 progressively decrease as the silica concentration increases. When the silica percentage was low, we observed a little rise in Al_2O_3 and K_2O, which gradually decreased as the silica level rose. The major Nyiragongo suite's relatively low MgO levels amply illustrate its highly fragmented composition. The high $Na_2O + K_2O$ (10.47 to 11.74) in the major suite indicates its extremely alkaline nature.

3.4.3 Magmatic affinities and evolutionary trend

The depletion of Fe in olivine is explained by the reduction of Mg in the magma that formed these lavas. The decreasing of titanium within the

magmatic liquid during differentiation is explained by the fact that in these two flows, the fractionation of ferrotitanium oxides occurs concurrently with the removal of ferromagnesian olivines. The flows from the eruptions in 2002 and 2021 have a strong affinity with the alkaline series on the TAS diagram. Since all of the samples fall into the domain of Foidite, the fundamental characteristics of these volcanics are justified. Based on these findings, Figure 14 shows the evolutionary trend of trace elements while accounting for silica concentration.

The inferences drawn from the key elemental evolutionary patterns are challenged by the geochemical evolution of suitable elements. Indeed, the concentration of silica in the magma leads to negative evolution of Cr, Ni, Zr, Ba, Sr, and Y. The differentiation of magma via fractional crystallization is justified by the depletion of Cr and Ni in the remaining liquid. The concentration of Rb in the lavas under study is nearly identical to that of Ba in nearly every sample examined. We see a decrease of Sr with increasing SiO_2 concentration. The Ni-SiO_2 figure illustrates how Ni is gradually depleted during magmatic differentiation.

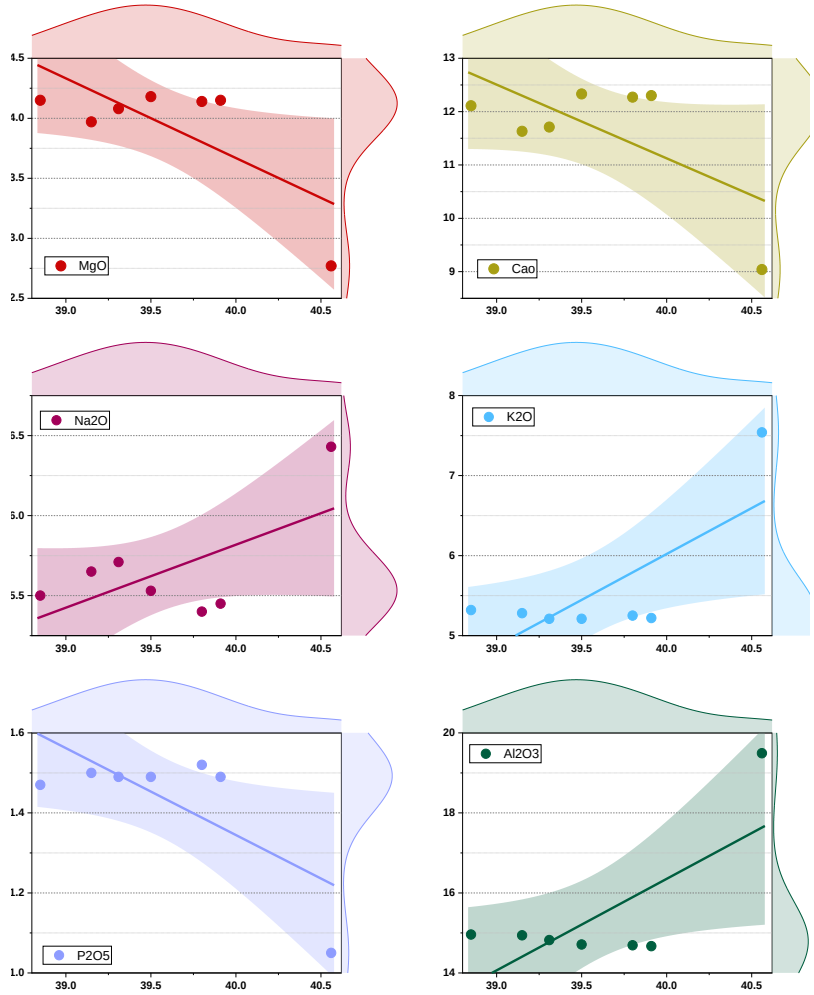

Figure 13: Major element (MgO, CaO, Na_2O, K_2O, P_2O_5, Al_2O_3) differences with regards to silica content in percentage (grouped marginal plot with linear regression)

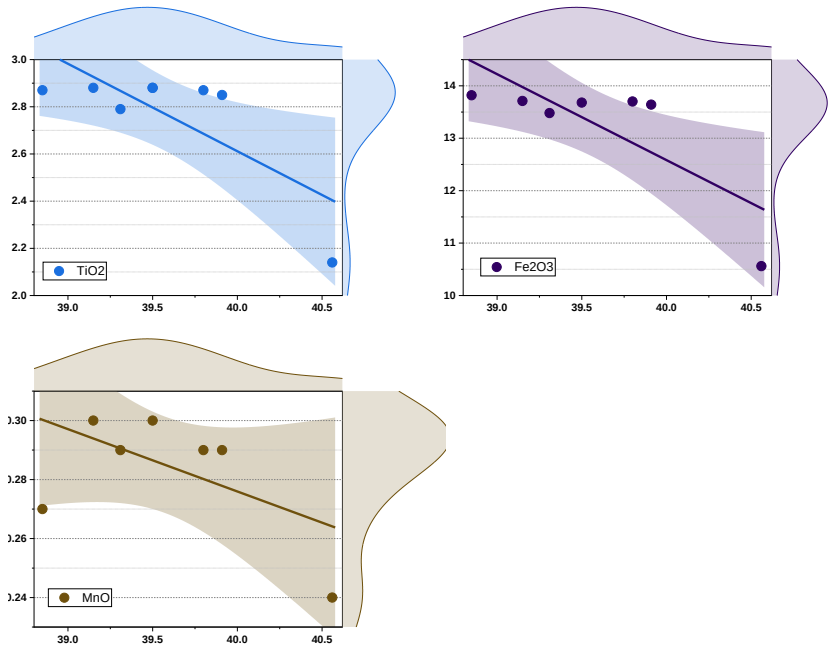

Figure 13: Continued (TiO_2, Fe_2O_3, MnO)

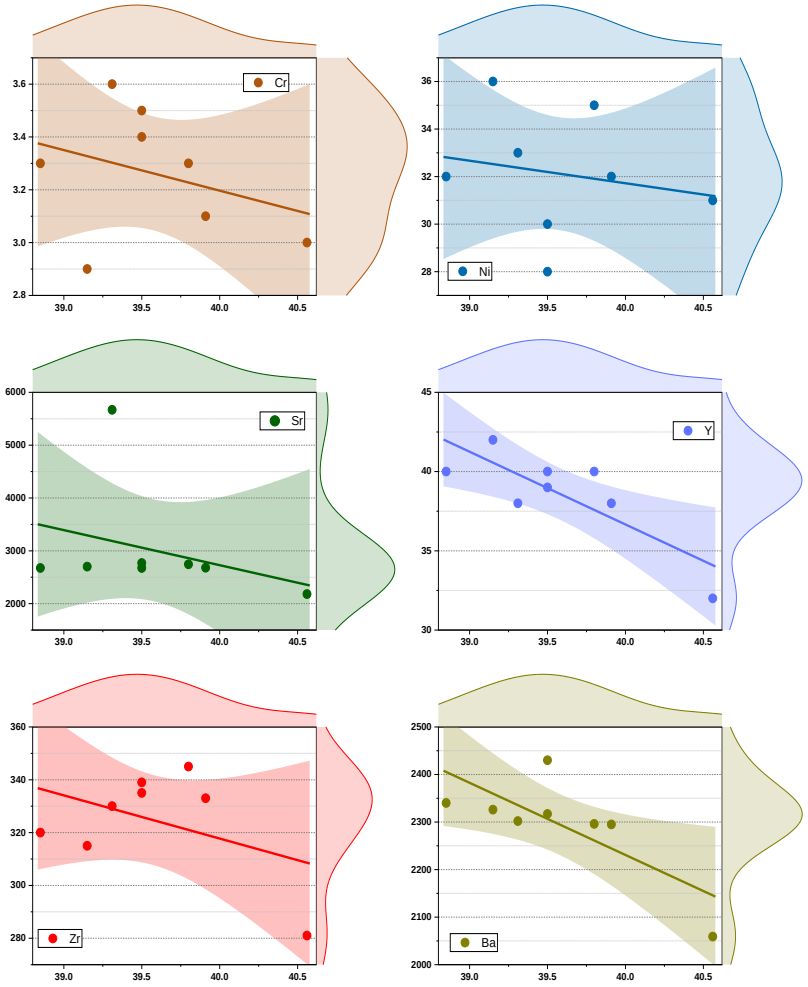

Figure 14: Trace element (in ppm) evolution trend depending on silica content (in percentage) with linear regression

3.4.4 Tectonic Site Geochemical Characterization

Various types of geotectonic sites may be distinguished using a variety of geochemical techniques (Pearce and Cann, 1973; Pearce and Norry, 1979; Wood et al., 1979). These techniques are based on the features of certain pairs of mismatched chemical elements (Zr/Y, Zr/Ti, Nb/Y, etc.) and on new theories of global tectonics. The proportions of these components seem typical for specific geotectonic locations, or even more accurately, of the sources situated above these locations. The writers mentioned above have created a number of discriminant diagrams by employing these components. Rebuilding their geotectonic framework is the goal of their utilization in old volcanic series.

Archean and modern mantles exhibit the same kind of heterogeneity, as demonstrated by Sun and Nesbitt's (1977) numerous similarities. They made claims that the proportions of several chemical elements (Al, Ca, Ti, Zr, Y, Yb, Sc, and V) in the Archean mantle and the mantle above oceanic ridges are same. The Archean mantle appears to include more of the other, more incompatible elements (La, Rb, Ba, and K). For instance, the Lan/Sm ratio in Archean volcanics ranges from 0.7 to 1.2, but it is about 0.55 in current N MORB-type tholeiites.

Following that, we identify the geochemical similarities between the 2002 and 2021 lavas and contemporary geotectonic locations using the discriminant diagrams (Figure 15) of Pearce and Cann (1973). There is a strong geochemical affinity between the lavas released by the Nyiragongo volcano during its recent eruptions and intra-plate basalt (WPB: Within Plate Basalt). Their features point to a deployment in the remote domain. The MgO–FeOt–Al_2O_3 diagram shown by Pearce et al. (1977) shows that every sample falls inside the continental area. In this instance, the East African Rift's wide (distensive) context, which is marked by lithosphere thinning and hot spot formation is the cause of the magma production. Hot spots' higher temperatures permit partial melting and the creation of magma. At this point, we discuss the rift's developmental background as it moves through the oceanization phase.

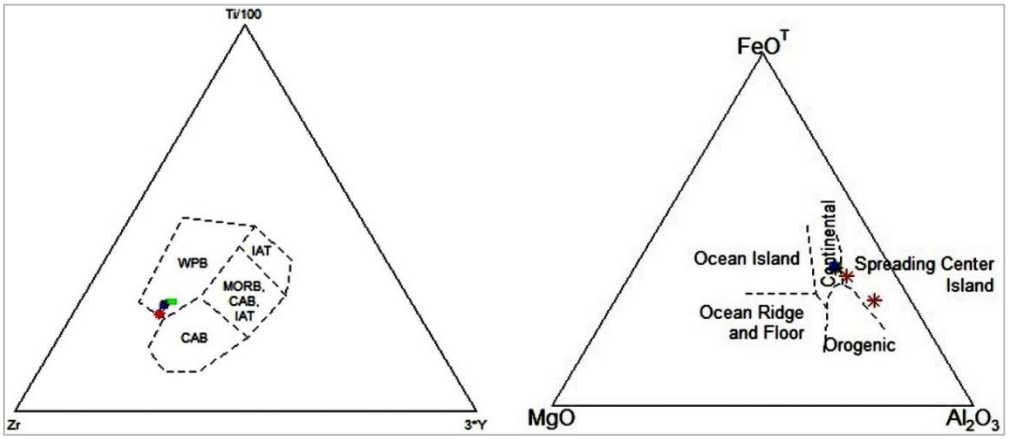

Figure 15: Discriminant diagrams (Pearce and Cann, 1973; Pearce et al., 1977)

4. Conclusion

This research aims to improve our understanding of the geology of the southern region of the Nyiragongo volcano, including its crater in Goma, Democratic Republic of Congo. It focuses on the geochemical and petrographic analyses of the volcano's flows from the 2002 and 2021 eruptions. The research focuses on lava flows from two previous eruptions in the region, which feature outcrops and an erratic sample matrix. The samples analyzed exhibit a geochemical relationship with alkaline-rich nephelinite, classified in the ultrabasic domain. The low content of Mg, Ca, and Fe in the samples reflects the lack of ferromagnesian and calcic minerals in thin sections. Magnesium, calcium, and iron concentrations were positively correlated with lava flows from the 2002 and 2021 eruptions.

5. Supplementary Information

5.1 Acknowledgments

We would like to take this opportunity to offer our appreciation to Albert Tienge ONGENDANGENDA, Ordinary Professor at University of Kinshasa.

5.2 Authors' Contributions

Conceptualization: IM; Design: IM; Investigation: NO; Project administration: NO & IM; Resources: NO; Software: NO & IM; Supervision: NO & IM; Validation: All authors; Visualization: All authors; Roles/Writing - original draft; NO & IM; Writing - review & editing: All authors.

References

Badriyo, A., G. Chazot, P. Kamgang. 2022. Pure forsterite in Nyiragongo lavas: evidence for subsolidus oxidation of volcanic rocks. Acta Geochim (2022) 41(1):12–23 https://doi.org/10.1007/s11631-021-00513-y

Burgi, G. Boudoire, F. Rufino, K. Karume, D. Tedesco. 2020. Recent Activity of Nyiragongo (Democratic Republic of Congo): New Insights From Field Observations and Numerical Modeling. Geophysical Research Letters, 2020, 47 (17), ff10.1029/2020GL088484ff. ffhal-02946391.

Chazot N, Willmott KR, Lamas G, Freitas AVL, Piron-Prunier F, Arias CF,Mallet J, De-Silva DL, Elias M. 2017. Renewed diversification followingMiocene landscape turnover in a Neotropical butterfly radiationbioRxiv 148189, http://dx.doi.org/10.1101/148189

Cole-Dai, J. 2010. Volcanoes and climate. Wiley Interdisciplinary Reviews: Climate Change, 1(6), 824-839. https://doi.org/10.1002/wcc.76

Ebinger, C., Sleep, N. 1998. Cenozoic magmatism throughout east Africa resulting from impact of a single plume. Nature 395, 788–791). https://doi.org/10.1038/27417

Ebinger, C.J. 1989. Tectonic development of the western branch of the East African rift system, Geological Society of America Bulletin 101 (7), pp885-903. https://doi.org/10.1130/0016-7606(1989)101<0885:TDOTWB>2.3.CO;2

Enrique, P., & Esteve, S. 2019. A chemical approximation to the modal QAPF and normative Q'(F')-ANOR classification of the igneous rocks based on their SiO2-CaO-K2O content. Geogaceta, 2019, vol. 66, p. 91-94.

Furman, T. & Graham, D., 1999, Erosion of lithospheric mantle beneath the East African Rift system: geochemical evidence from the Kivu volcanic province, Elsevier Lithos 48, pp237-262.

G. K. Sambo, K. Karume, C. B. Muhigirwa, H. Ciraba, M., T. M. Bibentyo, C. KA. Mahinda, A. K. Milungu, E. Kamate, K., F. K. Mukengere. 2016. Contribution to Geochemical study of geological formations of the Nyiragongo volcano: Case of the Lac Vert cone in Goma, North Kivu, DR Congo VL-15 IS-3 SP-685 EP-696 International Journal of Innovation and Applied Studies SN-20289324

Gregg, T. K. P. 2017. Patterns and processes: Subaerial lava flow morphologies: A review. Journal of Volcanology and Geothermal Research, 342, 3-12. https://doi.org/10.1016/j.jvolgeores.2017.04.022

H. De la Roche, J. Leterrier, P. Grandclaude, M. Marchal, 1980. A classification of volcanic and plutonic rocks using R1R2-diagram and major-element analyses — Its relationships with current nomenclature, Chemical Geology, Volume 29, Issues 1–4, Pp. 183-210, ISSN 0009-2541, https://doi.org/10.1016/0009-2541(80)90020-0.

Hamaguchi, H., Houlié, N., Kavotha, K. S., Lemarchand, A., Lockwood, J., Lukaya, N., Mavonga, G., de Michele, M., Mpore, S., Mukambilwa, K., Munyololo, F., Newhall, C., Ruch, J., · M. Yalire, M., & Wafula, M. 2002/2003. The January 2002 flank eruption of Nyiragongo volcano (Democratic Republic of Congo): chronology, evidence for a tectonic rift trigger, and major impact of lava flows on the city of Goma, «Acta Vulcanol.», Vol. 12 (1-2). 15 (1-2), pp 27-62.

Hirschn B., & Roussel, B. (Eds) 2009. Le Rift Est-Africain : Une singularité. Marseille: IRD Edition. DOI: 10.4000/books.irdeditions.1704

Jeffreys, H. 1925. The flow of water in an inclined channel of rectangular section. The London, Edinburgh, and Dublin Philosophical Magazine and Journal of Science,49(293), 793-807. https://doi.org/10.1080/14786442508634662

Kamate Kaleghetso, E. 2018. Pétrographie Et Géochimie Des Laves Du Volcan Nyiragongo (Nord Kivu, R. D. Congo) : Influence De La Viscosité Sur Les Paramètres De Propagation Des Coulées De Laves Menaçant La Ville De Goma. (Unpublished master's thesis). Université de Liège, Liège, Belgique. Retrieved from https://matheo.uliege.be/handle/2268.2/5534

Kamate, K. E. 2018. Pétrographie et géochimie des laves du volcan Nyiragongo (Nord Kivu, R. D. Congo) : Influence de la viscosité sur les paramètres de propagation des coulées de laves menaçant la ville de Goma. Université de Liège. http://hdl.handle.net/2268.2/5534

Le Bas, M.J., Le Maitre, R.W., Streckeisen, A. and Zanettin, B. 1986. A Chemical Classification of Volcanic Rocks Based on the Total Alkali-Silica Diagram. Journal of Petrology, 27, 745-750. https://doi.org/10.1093/petrology/27.3.745

Lev, E., & James, M. R. 2014. The influence of cross-sectional channel geometry on rheology and flux estimates for active lava flows.Bulletin of Volcanology, 76(829). https://doi.org/10.1007/s00445-014-0829-3

Marie, A. 2008. Vivre avec le volcan. Une géographie du risque volcanique au japon. Available online at: https://www.theses.fr/s18843

Michel Popoff, Du Gondwana à l'atlantique sud: les connexions du fossé de la bénoué avec les 1988. bassins du Nord-Est brésilien jusqu'à l'ouverture du golfe de Guinée au crétacé inférieur, Journal of African Earth Sciences (and the Middle East), Volume 7, Issue 2, Pages 409-431, ISSN 0899-5362, https://doi.org/10.1016/0899-5362(88)90086-3.

Middlemost, E.A.K. 1994. Naming Materials in the Magma/Igneous Rock System. Earth-Science Reviews, 37, 215-244. http://dx.doi.org/10.1016/0012-8252(94)90029-9

Minissale A., Donato A., Procesi M., Pizzino L., Giammanco S., 2019. Systematic review of geochemical data from thermal springs, gas vents and fumaroles of Southern Italy for geothermal favourability mapping, Earth-Science Reviews, Volume 188, 2019, Pages 514-535, ISSN 0012-8252, https://doi.org/10.1016/j.earscirev.2018.09.008

Mishina, M., 1983, Magnetotelluric Sounding in the Western Part of the Virunga Volcanic Region, volcanoes Nyiragongo and Nyamulagira: Gephysical aspects, Tohoku university, Sendai, Japan, pp75- 80.

Mishina, M., Zana, N. & Sawasawa, K. 1983. Geomagnetic Anomalies in the Virunga Volcanic Area and their Volcanological Implications, volcanoes Nyiragongo and Nyamulagira: Gephysical aspects, Tohoku university, Sendai, Japan, pp67-73.

Ongendangenda, A.T. 2012. Initiation à la pétrographie des laves des Virunga (R.D. Congo): avec un support de 92 photos de roches en lames minces 2012 Médiaspaul https://books.google.cd/books?id=ss8uoAEACAAJ

Pearce T.H., Gorman, B.E. and Birkett, T.C. 1977. The Relationship between Major Element Chemistry and Tectonic Environment of Basic and Intermediate Volcanic Rocks. Earth and Planetary Science Letters, 36, 121-132. http://dx.doi.org/10.1016/0012-821X(77)90193-5

Pearce, J.A. and Cann, J.R. 1973. Tectonic Setting of Basic Volcanic Rocks Determined Using Trace Element Analyses. Earth and Planetary

Science Letters, 19, 290-300. https://doi.org/10.1016/0012-821X(73)90129-5

Pearce, J.A. and Norry, M.J. 1979. Petrogenetic Implications of Ti, Zr, Y, and Nb Variations in Intrusive Rocks. Contributions to Mineralogy and Petrology, 69, 33-47. http://dx.doi.org/10.1007/BF00375192

Roberts, E. M., Stevens, N.J., O'Connor, P.M., Dirks, P.H.G.M., Gottfried, M.D., Clyde, W.C., Armstrong, R.A., Kemp, A.I.S. & Hemming, S. 2012. Initiation of the western branch of the East African Rift coeval with the eastern branch, Nature Geoscience 5, pp289-294. DOI: 10.1038/ngeo1432

Rosenthal, A., Foley, S. F., Pearson, D.G., Nowell, G.M. & Tappe, S. 2009. Petrogenesis of strongly alkaline primitive volcanic rocks at the propagating tip of the western branch of the East African Rift, Earth and Planetary Science Letters, Volume 284, Issues 1-2, pp236–248. https://doi.org/10.1016/j.epsl.2009.04.036

Rowland, S. K., & Walker, G. P. 1990. Pahoehoe and aa in Hawaii: volumetric flow rate controls the lavastructure. Bulletin of Volcanology, 52, 615–628. https://doi.org/10.1007/BF00301212

Sadaka K. Kavotha, Tuluka Mavonga, Jacques Durieux &Kibuye Mukambilwa. 2002. Towards a more detailed seismic picture of the January 17th. 2002. Nyiragongo eruption, Acta Vulcanologica. Vol. 12 (1-2), 2002. 15 (1-2), 2003, pp87-100.

Saemundsson, « *East African Rift System-An Overview* », Reykjavik: United Nations University, Iceland GeoSurvey, 2009.

Sarah Colclough, 2005, Investigations of Nyamulagira and Nyiragongo volcanoes (DRC) using interferometric synthetic Apperture, Radar, Thesis, Christ's College, 194p.

Siebert, L., Simkin, T., & Kimberly, P. (2011). Volcanoes of the World. Univ of California Press.

Smets, B., D'Oreye, N., Kervyn, M. & Kervyn, F. 2017. Gas piston of the Nyiragongo lava lake: First insights from a stereographic Time-Lapse-Camera system, Journal of African Earth Sciences, Volume 134, pp874-887. https://doi.org/10.1016/j.jafrearsci.2016.04.010

Sun S. S., Nesbitt R.W. 1977. Chemical heterogeneity of the Archean mantle composition of the bulkearth and mantle evolution. Earth Planet Sci Lett 35:429–448.

Taylor, C.D., Schulz, K.J., Doebrich, J.L., Orris, G.J., Denning, P.D., and Kirschbaum, M.J., 2009, Geology and nonfuel mineral deposits of Africa and the Middle East: U.S. Geological Survey Open-File Report 2005–1294-E, 246 p.

Tiercelin, J. J., Scholz, C. A., Mondeguer, A., Rosendahl, B. R., & Ravenne, C. (1989). Discontinuites sismiques et sedimentaires dans la serie de remplissage du fosse du Tanganyika, Rift Est-africain. *Comptes Rendus - Academie des Sciences, Serie II*, *309*(16), 1599-1606.

Wauthier, C., Cayol, V., Kervyn, F. & d'Oreye, N. 2012. Magma sources involved in the 2002 Nyiragongo eruption, as inferred from an InSAR analysis, journal of geophysical research, vol. 117, B05411. https://hal.science/hal-00793989/document

Wood, S. D., Joron, J. J., Trueil, M., Norry, M. & Tarney, J. 1979. Elemental and Sr isotope variations in basic lavas from Iceland and surrounding ocean floor. The nature of mantle source heterogeneities. Contributions to Mineralogy and Petrology 70, 319–340.